Food Research International 54 (2013) 195–202

Contents lists available at ScienceDirect

Food Research International

journal homepage: www.elsevier.com/locate/foodres

Formation and functionality of soluble and insoluble electrostatic complexes within mixtures of canola protein isolate and (κ-, ι- and λ-type) carrageenan

Andrea K. Stone, Lamlam Cheung, Chang Chang, Michael T. Nickerson *

Department of Food and Bioproduct Sciences, University of Saskatchewan, 51 Campus Drive, Saskatoon, SK S7N 5A8, Canada

ARTICLE INFO

Article history:
Received 15 April 2013
Accepted 6 June 2013

Keywords:
Canola protein
Complex coacervation
Carrageenan
Functionality

ABSTRACT

The formation of electrostatic complexes between a canola protein isolate (CPI) and (κ-, ι-, and λ-type) carrageenan (CG) was investigated as a function of pH (1.50–7.50) and biopolymer weight mixing ratio (1:1–75:1, CPI–CG) by turbidimetric measurements during an acid titration. The addition of CG to CPI suppressed CPI–CPI aggregation. Critical pHs designating structure forming events (pH_c, $pH_{\phi 1}$ — soluble and insoluble complexes, respectively) shifted to more acidic pHs as the mixing ratio increased then plateaued at the 15–20:1 ratio. The functional properties (solubility, foaming capacity/stability, emulsion capacity, emulsion stability) of the complexes (20:1, CPI–CG) at pH_c (6.75) and $pH_{\phi 1}$ (5.00) were compared to CPI alone. At both pHs, solubility, foaming capacity and emulsion capacity of CPI were reduced upon complexation with CG. Emulsion stability of the complexes was high at ~87–96% depending on pH and CG type. Differences in functionality based on CG type were related to the structure and charge of the CG molecules. The pH of net neutrality was reduced from pH 5.78 for CPI alone to pH 5.35 for CPI–κ-CG and pH 4.95 for both CPI–κ-CG and CPI–ι-CG.

1. Introduction

Protein and polysaccharides are widely used by the food industry for their functionality and ability to control food structure (Schmitt & Turgeon, 2011; Tolstoguzov, 2002; Ye, 2008). Their interactions can also be carefully tailored for protein separation/purification purposes (Xu, Mazzawi, Chen, Sun, & Dubin, 2011) or in the design of biopolymer adhesives, edible films (Schmitt, Sanchez, Desobry-Banon, & Hardy, 1998) and controlled delivery applications (Schmitt & Turgeon, 2011). A better understanding of biopolymer interactions and factors/conditions leading to their phase behavior could increase their usefulness for tailoring food structure or in the development of more high value applications (e.g., capsules and films).

Mixtures of proteins and polysaccharides generally exhibit either segregative or associative phase behavior due to the electrostatic forces arising between the two (Schmitt et al., 1998; Tolstoguzov, 2002; Ye, 2008). Segregative phase behavior is the result of electrostatic repulsive forces between similarly charged biopolymers, leading to separation into both a protein-rich and a polysaccharide-rich phase (Boral & Bohidar, 2010; Schmitt & Turgeon, 2011; Schmitt et al., 1998; Tolstoguzov, 1991). In contrast, associative phase behavior (also known as complex coacervation) occurs with biopolymers of opposing net charges through primarily electrostatic attractive forces, with secondary stabilization by hydrogen bonding (Liu, Elmer, Low, & Nickerson, 2010). Complex coacervation leads to both a biopolymer-rich and a solvent-rich phase (Boral & Bohidar, 2010; Schmitt & Turgeon, 2011; Schmitt et al., 1998; Tolstoguzov, 1991). The biopolymer-rich phase consists of soluble and insoluble complexes that re-orient into either a coacervate or precipitate-type morphology depending on the strength of the polyelectrolytes present. Coacervates are comprised of complexed biopolymers, typically involving a strong (e.g., protein) and weakly (e.g., gum Arabic) charged polyelectrolyte, which entrap small amounts of solvent to remain quite mobile (Klassen, Elmer, & Nickerson, 2011). In contrast, complexes that precipitate typically involve mixtures with both strongly charged proteins and polysaccharides, such as carrageenan, alginate, chitosan and pectin, and tend to form over a much narrower pH range before precipitating out of solution. Complexation in either case is driven by a loss in entropy associated with conformational freedom and solvent mixing, which offsets the enthalpic contribution from the release of counterions and water (Boral & Bohidar, 2010; Liu, Low, & Nickerson, 2009).

Due to the electrostatic nature of complexation, biopolymer interactions are strongly influenced by solvent properties, such as pH, temperature and ionic strength; biopolymer characteristics, such as molecular weight, charge density, distribution/type of reactive sites, conformation, and hydration; and mixing conditions, such as biopolymer mixing ratio and, level and duration of shear processing (Schmitt et al., 1998; Semenova, Pavlovskaya, & Tolstoguzov, 1991; Ye, 2008). Typically, researchers study associative phase behavior during a turbidimetric

* Corresponding author at: Department of Food and Bioproduct Sciences, University of Saskatchewan, 51 Campus Drive, Saskatoon, SK S7N 5A8, Canada. Tel.: +1 306 966 5030; fax: +1 306 966 8898.
E-mail address: Michael.Nickerson@usask.ca (M.T. Nickerson).

0963-9969/$ – see front matter © 2013 Elsevier Ltd. All rights reserved.
http://dx.doi.org/10.1016/j.foodres.2013.06.009

pH-titration, in which multiple pH-induced structure forming events can be observed. For instance, in mixtures of proteins and an anionic polysaccharide at solvent pH higher than the protein's isoelectric point (pI), the system is co-soluble (under dilute biopolymer conditions). However, as pH is lowered below the pI, the protein takes on a positive net charge and begins to experience electrostatic attraction with the negatively charged polysaccharide. Initial interactions, first experimentally detected by an inflection point in the turbidity–pH profile signify the formation of soluble complexes (denoted by the critical pH, pH_c). As the solution is acidified further, a dramatic rise in turbidity occurs corresponding to macroscopic phase separation and the formation of insoluble complexes (denoted by the critical pH, $pH_{\phi 1}$) (Liu et al., 2009; Weinbreck, Nieuwenhuijse, Robjin, & de Kruif, 2004; Xia & Dubin, 1994). Complexation becomes greatest once biopolymers reach an electrical equivalence point to become electrically neutral (denoted by maximum turbidity vs. pH at pH_{opt}) (Liu et al., 2009). Complex formation then becomes weaker at $pH < pH_{opt}$ until complete dissolution occurs (denoted by the critical pH, $pH_{\phi 2}$), where the reactive sites on the polysaccharide become protonated. If complexation leads to precipitate formation, only pH_c and $pH_{\phi 1}$ may be determined, and structures begin to fall out of solution near pH_{opt} creating scattering in the O.D. vs. pH data at lower pHs. In some cases involving two highly charged biopolymers, initial interactions can occur at pH > pI where they have similar net charges thought to be due to surface patch binding or interactions between negatively charged polysaccharides and positively charged patches on the protein's surface (Boral & Bohidar, 2010; Gupta, Bohidar, & Aswal, 2007).

Canola protein isolate (CPI) is typically extracted from canola meal, which is a protein-rich (≤50%, dry basis) by-product of canola oil extraction that is most commonly used for animal feed (Aider & Barbana, 2011; Uruakpa & Arntfield, 2005; Wu & Muir, 2008). However because of canola protein's well balanced amino acid profile and functionality, it is increasingly being investigated for its potential as a new food ingredient (Aider & Barbana, 2011). Canola proteins consist of two major storage proteins, cruciferin and napin. Cruciferin, is a 12 S hexameric globulin protein (~300 kDa) containing 6 subunits (~50 kDa), with each comprising of two polypeptide chains (α-chain, 30 kDa; β-chain 20 kDa) joined by a disulfide bond (Aider & Barbana, 2011; Lampart-Szczapa, 2001). In contrast, napin is a 2 S albumin with low molecular weight (12–14.5 kDa) and two polypeptide chains (4.5 and 10 kDa) linked primarily by disulfide bonds (Berot, Compoint, Larre, Malabat, & Gueguen, 2005; Monsalve & Rodriguez, 1990).

Carrageenan (CG) is an anionic linear sulfated polysaccharide derived from red algae (*Rhodophyceae*) and is commonly used in the food industry for gelling and thickening applications (Clark & Ross-Murphy, 1987). Structurally it is comprised of partially sulfated repeating (1–3) linked β-D-galactose and (1–4) linked 3,6-anhydro-α-D-galactose residues (Clark & Ross-Murphy, 1987). The three main classes of CG, κ-, ι-, and λ-types, are based on the number of sulfate groups (1, 2 and 3, respectively) per repeat unit. Kappa- and ι-CG exist as random coils at sufficiently high temperatures and undergo a disordered–ordered transition when the temperature is reduced resulting in a double helical structure (Morris, Rees, & Robinson, 1980). Side-by-side aggregation of the helices, and subsequent gelation, occurs in the presence of gel-promoting salts (Morris et al., 1980). Kappa- and ι-CG are known to have different salt sensitivities in respect to gelation, κ-CG is K^+ sensitive with an intramolecular bridge forming between K^+ and the sulfate group of D-galactose and the K^+ and the anhydro-O-3,6 ring of the second D-galactose unit, through an ionic bond and electrostatic association, respectively (te Nijenhuis, 1997). Calcium promotes gelation more than other cations in ι-CG. This specificity involves intramolecular bridging between the two sulfate groups of the same repeat unit through ionic forces with Ca^{2+} and intermolecular bridging between sulfate groups of different residues through ionic and electrostatic forces with Ca^{2+} (te Nijenhuis, 1997). It was believed that λ-CG does not have gelation abilities but forms only viscous solutions due to its high linear charge density and lack of an ordered conformation (Piculell, 2006; te Nijenhuis, 1997; Weinbreck et al., 2004).

Complexation studies involving plant proteins and polysaccharides are limited compared to those systems involving animal-derived proteins in the literature. In addition, although there are a few studies relating the functionality of mixed complexed biopolymer systems (Gu, Decker, & McClements, 2005; Liu, Elmer, Low, & Nickerson, 2010; Schmidt, Novales, Boue, & Axelos, 2010; Stone & Nickerson, 2012), very few studies compare both soluble and insoluble complex functionalities. Klassen et al. (2011) investigated complex formation involving CPI with alginate and ι-CG under various pHs and mixing ratio conditions, and also studied the impact of complexation on protein solubility as a function of pH. In both mixtures, complexation leads to the formation of precipitate-type structures, with only the CPI–alginate mixture experiencing improved solubility near CPI's pI. The present study focuses on understanding the effects of pH and biopolymer mixing conditions on the formation of soluble and insoluble electrostatic complexes involving a canola protein isolate and (κ-, ι-, and λ-type) carrageenan (CG); as well as the resulting functional attributes of the formed complexes relative to CPI alone.

2. Materials and methods

2.1. Materials

Canola seeds (SP Desirable *Brassica napus*, Lot#: 168-8-129810) were kindly provided by Viterra (Saskatoon, SK, Canada), whereas κ-, ι- and λ-type CG were purchased from Sigma-Aldrich Canada Ltd. (Oakville, ON, Canada). Canola protein isolate was prepared according to the defatting protocol and salt extraction method of Folawiyo and Apenten (1996) as previously described (Klassen et al., 2011). Chemical analyses of the materials found CPI to be comprised of 95% protein (N × 5.70), 0.70% moisture, 0.32% lipid, 2.32% ash and 1.71% carbohydrate as determined by Association of Official Analytical Chemists (AOAC, 2003) methods; 925.10 (moisture), 923.03 (ash), 920.87 (crude protein), and 920.85 (lipid). Carbohydrate content was determined on the basis of percent differential from 100%. In the case of CG, the κ-type was comprised of 66.50% carbohydrate, 10.65% moisture and 22.86% ash (including: 2.4% Ca^{2+}, 0.16% Mg^{2+}, 5.4% K^+ and 0.49% Na^+); ι-type was comprised of 64.40% carbohydrate, 10.82% moisture and 24.97% ash (including: 3.4% Ca^{2+}, 0.18% Mg^{2+}, 3.2% K^+ and 1.2% Na^+); and the λ-type comprised of 63.79% carbohydrate, 12.26% moisture and 23.95% ash (including: 3.0% Ca^{2+}, 0.83% Mg^{2+}, 2.4% K^+ and 1.3% Na^+). In all cases, protein and lipid contents were considered to be negligible. All chemicals used in this study were of reagent grade and purchased from Sigma-Aldrich (Oakville, ON, Canada).

2.2. Turbidimetric pH-acid titrations

Critical pH values (pH_c and $pH_{\phi 1}$) associated with the formation of soluble and insoluble complexes within CPI–CG mixtures were investigated by turbidimetric pH acid titrations as a function of pH (7.50–1.50) and biopolymer mixing ratio (1:1–35:1; CPI:CG) at a constant biopolymer concentration of 0.05% (w/w). CPI and CG solutions were prepared by dissolving each powder in Milli-Q water at pre-determined mixing ratios and stirring for 2 h at room temperature (~21–23 °C) before adjusting solutions to pH 8.00 using 0.5 M NaOH. Solutions were then allowed to stir overnight at 4 °C to help facilitate solubility. Optical density measurements were made at room temperature over a pH range (7.50 to 1.50) using a UV/vis spectrophotometer (Thermo Scientific, Waltham, MA) at 600 nm using plastic cuvettes (1 cm path length). The pH of the solutions was lowered by drop wise addition of HCl using a gradient of HCl concentrations (0.05 M > pH 6.00; 0.1 M > pH 3.50; 0.5 M > pH 3.00; 1 M > pH 2.50 and 2 M > pH 1.50) to reduce dilution effects associated with the titration (i.e., <3 mL of HCl was added to 100 g of solution upon completion of the titration). Turbidity measurements

were made on individual CPI and CG solutions (0.05% w/w) as controls. Critical pH values associated with structure forming events were determined graphically on individual turbidity curves as described by Weinbreck, Nieuwenhuijse, Robijn, and de Kruif (2003) and Liu et al. (2009). All measurements were made in triplicate.

2.3. Electrophoretic mobility

Electrophoretic mobility (U_E) (i.e., velocity of a particle within an electric field) for individual and mixed CPI–CG (20:1 CPI–CG mixing ratio) solutions (0.05% w/w — total biopolymer concentration) was measured as a function of pH (7.00–2.00) using a Zetasizer Nano-ZS90 (Malvern Instruments, Westborough, MA). Samples were prepared and acidified as previously described in Section 2.2. Measurements were made every one pH increment and were performed in duplicate. Electrophoretic mobility was used to calculate the zeta potential (estimate of surface charge on biopolymer, ζ) using the Henry equation:

$$U_E = \frac{2\varepsilon \times \zeta \times f(\kappa\alpha)}{3\eta} \quad (1)$$

where η is the dispersion viscosity, ε is the permittivity, and $f(\kappa\alpha)$ is a function related to the ratio of particle radius (α) and the Debye length (κ). Using the Smoluchowski approximation $f(\kappa\alpha)$ equalled 1.5.

2.4. Functional properties of electrostatic complexes

Functional properties of CPI–CG mixtures (20:1 CPI–CG mixing ratio) were determined at a 1% (w/w) total biopolymer concentration at pHs 6.75 and 5.00 corresponding to where soluble and insoluble complexes exist, respectively (described in Section 3.1—Results and discussion and Fig. 3). Individual CPI solutions were also tested at corresponding pHs and concentrations as the mixed systems. Unless otherwise stated, samples were prepared in a similar manner as described in Section 2.2. All measurements were performed in triplicate.

2.4.1. Protein solubility

The solubility of CPI–(κ-, ι- and λ-type) CG complexes and individual CPI solutions were determined by a modified method of Morr et al. (1985) at pHs 6.75 and 5.00. CPI and CG powders were dissolved in 0.1 N NaCl. Solutions were allowed to stir (500 rpm) for 1 h at the desired pH to facilitate the formation of complexes, then centrifuged (Sorvall® SS-1 Superspeed Angle Centrifuge, DJB Labcare Ltd., England) at 1000 ×*g* for 10 min at room temperature. Protein content of the supernatant was determined by micro-Kjeldahl (%N × 5.7) analysis. Percent protein solubility was determined by dividing the protein content of the supernatant by the total sample protein content.

2.4.2. Foaming capacity and stability

Foaming capacity (FC) and stability (FS) were determined according to modified methods of Liu, Elmer, Low, and Nickerson (2010). In a 400 mL beaker (inner diameter = 69 mm; height = 127 mm; as measured by a digital caliper) 15 mL (V_{li}, initial volume of liquid used to make foam) of biopolymer solution at the required pH was foamed at 8000 rpm using an Omni Macro homogenizer (Omni International Inc., Marietta, GA) equipped with a 20 mm diameter saw tooth generating probe (positioned slightly below the air–water interface) for 5 min. Immediately following homogenization, the foam was transferred to a 100 mL graduated cylinder (inner diameter = 26 mm; height = 25 cm). Foam capacity and FS were determined using Eqs. (2) and (3), respectively, where V_{fi} is the volume of foam immediately after homogenization and V_{ft} is the volume of foam remaining after time. Foaming stability was determined after 30 min.

$$\%FC = \frac{V_{fi}}{V_{li}} \times 100\% \quad (2)$$

$$\%FS = \frac{V_{ft}}{V_{fi}} \times 100\%. \quad (3)$$

2.4.3. Emulsion stability

Emulsion stability (ES) was determined for 50/50 (5 mL canola oil/5 mL biopolymer solution (V_B)) oil-in-water emulsions (Stone & Nickerson, 2012). Emulsions were prepared in 50 mL screw capped plastic centrifuge tubes and were homogenized for 5 min at 8000 rpm with the Omni Macro homogenizer equipped with a saw tooth generating probe, positioned at the oil–water interface. Emulsions were then transferred to 10 mL graduated cylinder (inner diameter = 10.80 mm; height = 100.24 mm; as measured by a digital caliper) and allowed to separate for 30 min. Emulsion stability was determined using Eq. (4) where V_A is the volume of the aqueous layer after 30 min of drainage.

$$\%ES = \frac{V_B - V_A}{V_B} \times 100\%. \quad (4)$$

2.4.4. Emulsion capacity

Two grams of biopolymer solution along with canola oil (3–5 g) was added to 50 mL centrifuge tubes to obtain a series of emulsions with varying amounts of oil. Immediately after homogenization of each emulsion (5 min, 8000 rpm, Omni Macro Homogenizer equipped with a saw tooth generating probe), conductivity was measured using an Orion 3-star conductivity meter with a 4-electrode conductivity cell (Thermo Scientific, Waltham, MA, USA). Emulsion capacity (EC) was determined at the inversion point when an oil-in-water emulsion changed to a water-in-oil emulsion as indicated by a large drop in emulsion conductivity. Emulsion capacity was expressed as g oil emulsified per g protein as the average oil amount before and after the inversion.

2.5. Statistics

A one-way analysis of variance (ANOVA) with Scheffe's post-hoc test was used to measure statistical differences within state diagrams for each critical pH value as a function of biopolymer mixing ratio and to measure statistical differences within soluble complexes and insoluble complexes functionality. All statistical analyses were performed using Systat software (SPSS Inc., Ver. 10, 2000, Chicago, IL).

3. Results and discussion

3.1. Effect of pH and mixing ratio on the formation of electrostatic complexes

Optical density (OD) for individual solutions of canola protein isolate (Fig. 1) and (κ-, ι- and λ-type) CG (not shown) was investigated during a pH acid titration between pH 7.00 and 1.50. The turbidity profile for CPI followed a bell-shaped profile with a rapid rise in OD initiating at pH 7.00, until reaching a maximum (near OD 0.970) at pH 5.60, and then declining in magnitude to pH 3.50 below which minimal OD was observed (Fig. 1). Klassen et al. (2011) found a similar bell shaped profile for salt extracted CPI. The rise in OD is thought to be associated with CPI–CPI aggregation which is strongest near the protein's pI where electrostatic charge repulsion is reduced significantly between neighboring molecules. As the OD of the CPI solution increases it is thought that the size and number of CPI–CPI aggregates are increasing. No OD was observed for the carrageenan materials over the pH range 7.00–1.50 (data not shown).

In the mixed CPI–CG system the addition of CG (regardless of CG-type) resulted in significant suppression of CPI–CPI aggregation relative to the individual CPI system as seen by substantially reduced OD in the mixed systems and a shift in initial OD rise during the acid titration towards more acidic pHs (Fig. 2). Both of these trends were less

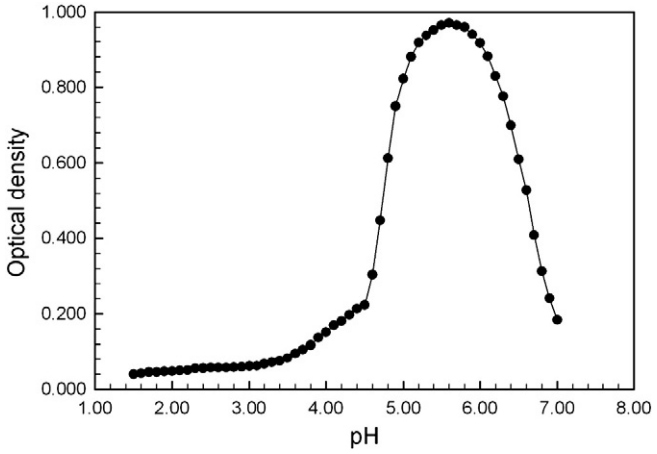

Fig. 1. Mean turbidity curve for an individual homogenous CPI solution as a function of pH (n = 3).

pronounced as the concentration of CG was decreased, i.e. as mixing ratio increased. For the 1:1 CPI–(κ-, ι- and λ-type) CG system, OD data as a function of pH was relatively flat, with maximum OD occurring at <0.150 indicating very little CPI–CPI aggregation was occurring (Fig. 2). Suppression of CPI–CPI aggregation was thought to be associated with the presence of strong electrostatic forces arising from sulfate groups along the CG backbone of free molecules in solution.

At higher mixing ratios, critical pHs associated with the formation of soluble and insoluble complexes were found to occur at pHs all above the pI of CPI, where both biopolymers carried a net negative charge (Figs. 2 and 3). In all cases, complex formation led to the formation of precipitate-type structures, which began to fall out of solution soon after the maximum OD was reached (note; data corresponding to pHs where precipitation occurred was removed from Fig. 2). In contrast to a coacervate morphology, precipitates are more compact, entrap less solvent and tend to be irreversible. This initial electrostatic attraction (denoted by pH_c) between the two biopolymers at pH > pI is presumed to be associated with the interaction of CG molecules with positively charged patches distributed on the protein's surface (de Vries, Weinbreck, & de Kruif, 2003; Dickinson, 1998; Weinbreck et al., 2004). This has previously been reported in several systems including whey protein isolate (WPI)–CG (Stone & Nickerson, 2012; Weinbreck et al., 2004) and, CPI–alginate and CPI–ι-CG (Klassen et al., 2011).

For all mixed systems (with the exception of the 1:1 mixing ratio), pH_c and $pH_{\phi 1}$ shifted to higher pHs as the mixing ratio increased (i.e., less CG is present at higher ratios), until nearing a plateau at a 20:1 CPI–CG ratio, with the exception of pH_c for κ-CG which plateaued at the 15:1 ratio (Fig. 3). The mixing ratio dependence suggests the presence of CPI–CPI aggregates participating with complex formation, where it was hypothesized that aggregates increased in size as the mixing ratio increased up to a critical point (corresponding to the plateau region of the curve). Similar findings were reported for mixtures of pea protein isolate–gum Arabic (Liu et al., 2009), pea protein–alginate (Klemmer, Waldner, Stone, Low, & Nickerson, 2012), gelatin–agar (Singh et al., 2007) and CPI–alginate/ι-CG (Klassen et al., 2011). Weinbreck et al. (2004) and Girard, Sanchez, Laneuville, Turgeon, and Gauthier (2004) investigated complexation within WPI–CG and β-lactoglobulin–pectin mixtures, respectively, using protein solutions where aggregates were pre-filtered prior to complexation. Both authors reported the absence of mixing ratio dependence of pH_c, where they hypothesized that complexation involved individual proteins and polysaccharide molecules. In the case of $pH_{\phi 1}$, mixing ratio dependence was observed for both systems which was thought to be attributed to an increase in the number of proteins interacting with the same number of polysaccharide chains.

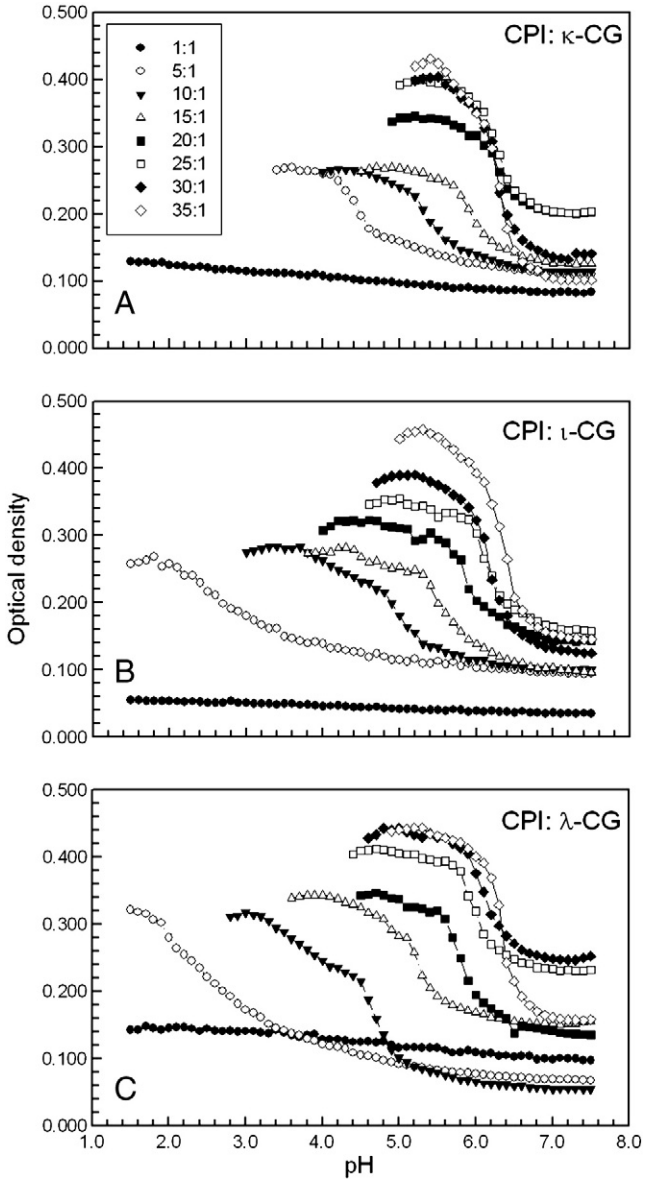

Fig. 2. Mean turbidity curves for CPI–κ-GG (A), CPI–ι-CG (B), and CPI–λ-CG (C) mixtures as a function of pH and biopolymer mixing ratios (n = 3).

At the 20:1 CPI–CG mixing ratio, the size of complexes was presumed to be similar involving κ- and λ-type CG as the maximum OD was similar (OD ~0.350), whereas the maximum OD reading involving the ι-type CG was lower (~0.326) (Fig. 2). Differences in the maximum OD readings as a function of CG-type are presumed to be associated with the structure of the various CG molecules in solution, and how this then impacts the formation of complexes. For instance, the number of sulfate groups available for complexation with CPI increases from 1, 2 and 3 per disaccharide repeat unit for κ-, ι- and λ-type CG, respectively; and the ordered conformation of CG differs at room temperature where both κ- and ι-types form double helical structures whereas λ-type remains in a random coil. CG conformation will impact chain flexibility and the amount of exposed reactive sites available for complexation with CPI. Stone and Nickerson (2012) reported that within WPI–(κ-, ι- and λ-type) CG mixtures, the ι-type had the greatest effect on inhibiting complex formation, where maximum complexation was found to occur at a 20:1 WPI–CG mixing ratio versus a 12:1 ratio for the κ- and λ-CG types. The authors hypothesized that although λ-CG has a greater number of sulfate groups per repeat unit than ι-type, its ability to inhibit CPI–CPI aggregation was less since λ-CG remained in

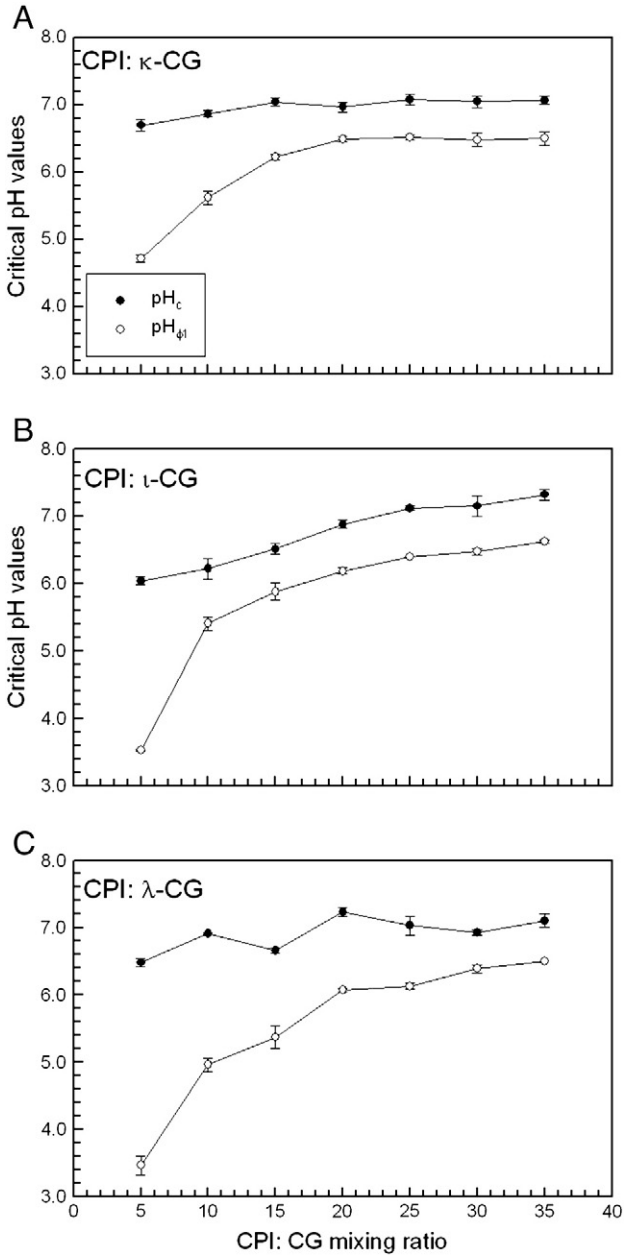

Fig. 3. Critical pH values associated with the formation of soluble (pH_c) and insoluble ($pH_{\phi 1}$) complexes within admixtures of CPI–κ-GG (A), CPI–ι-CG (B), and CPI–λ-CG (C) mixtures as a function of biopolymer mixing ratios. Data represent the mean ± one standard deviation.

a random coil conformation (rather than double helical structure), and as such, may not have all sulfate groups available for binding with the protein. Gu et al. (2005) concluded that magnitude of electrostatic interactions between the three CG types and β-lactoglobulin was influenced not just by the relative charge density of the CGs but also by the CG conformation.

Electrophoretic mobility was measured for 20:1 CPI–CG mixtures and individual solutions of CPI and CG as a function of pH (7.00–1.50) (Fig. 4). The individual CPI solution indicated its pI value to be at a pH of 5.78 (Fig. 4), corresponding closely to where the CPI turbidity curve peaked (pH 5.60) (Fig. 1). In contrast, individual CG molecules, regardless of their type remained highly negatively charged (~−40 to −80 mV) over the entire pH range (Fig. 4). The pI for CPI in the present study was lower than typically reported in the literature for cruciferin (pI 7.2) and napin (pI ~11.0), which are usually determined based on their amino acid composition. In the present study, pI is determined based on the electrophoretic mobility of the protein in solution. CPI constitutes a mixture of proteins, which are most likely experiencing some level of aggregation which exposes some, and buries other amino acids from the surface to influence mobility. Where mobility ceases, CPI displays no net charge (zeta potential = 0 mV). In the mixed systems, the presence of CG shifted the pH of net neutrality to more acidic pHs relative to the individual CPI system due to the complexation of CG molecules to the CPI–CPI aggregate surface. Mixtures of both CPI–ι-CG and CPI–λ-CG shifted net neutrality to occur at pH 4.95, whereas in the case of CPI–κ-CG, net neutrality shifted to only pH 5.35. A similar trend was found for WPI–CG complexes with WPI–κ-CG having a higher pH of net neutrality compared to WPI mixed with ι- or λ-CG. Klassen et al. (2011) reported CPI–ι-CG complexes having net neutrality at pH 4.55 which was consistent with our findings.

3.2. Functional properties of soluble and insoluble CPI–CG complexes vs. CPI alone

3.2.1. Solubility

The functional properties of CPI and CPI–CG mixtures were investigated at pH 6.75 and 5.00 corresponding to pH conditions where soluble and insoluble complexes, respectively, were present in solution (Table 1). 'Insoluble complexes' refer to terminology associated with the protein–polysaccharide complex occurring and not its functional properties; solubility of said complexes refers to how much of the complex can remain suspended in solution. At pH 6.75, solubility

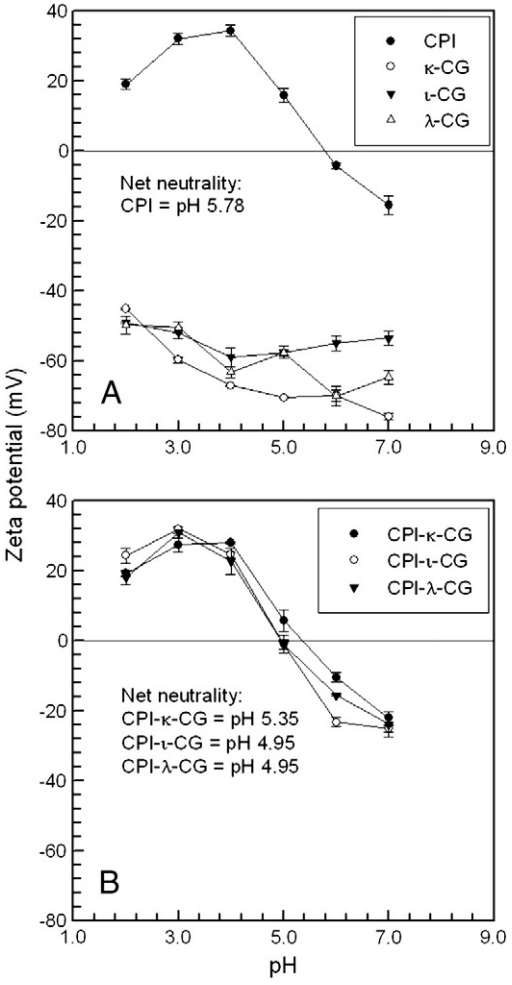

Fig. 4. Surface charge (zeta potential, mV) of homogenous (CPI and κ-, ι- and λ-type CG) (A) and mixed (CPI–(κ-, ι- and λ-type) CG, 20:1 ratio) (B) biopolymer solutions (20:1 mixing ratio) as a function of pH. Data represent the mean ± one standard deviation.

Table 1
Functional attributes of canola protein isolate (CPI)–(κ-, ι- and λ-type) carrageenan (CG) mixtures under biopolymer (20:1 CPI–CG mixing ratio) and pH conditions where soluble and insoluble complexes exist. Data represent the mean ± one standard deviation (n = 3).

	Solubility (%)	Foaming capacity (%)	Foaming stability (%)	Emulsion stability (%)	Emulsion capacity (g/g)
Soluble complexes (pH 6.75)					
CPI–κ-CG	84.27 ± 2.37	144.44 ± 10.18	69.95 ± 3.42	91.67 ± 5.13	194.69 ± 7.58
CPI–ι-CG	68.35 ± 2.29	120.00 ± 5.77	70.87 ± 0.98	96.00 ± 2.00	190.31 ± 0.00
CPI–λ-CG	61.90 ± 5.74	111.11 ± 3.85	64.40 ± 4.88	87.33 ± 3.06	164.06 ± 0.00
CPI (control)	96.50 ± 0.44	271.11 ± 10.18	74.20 ± 0.70	86.00 ± 2.00	225.31 ± 7.58
Insoluble complexes (pH 5.00)					
CPI–κ-CG	47.46 ± 1.19	97.78 ± 3.85	81.75 ± 4.32	96.00 ± 0.00	181.56 ± 15.16
CPI–ι-CG	61.89 ± 0.54	71.11 ± 3.85	77.88 ± 6.82	94.67 ± 2.31	190.31 ± 13.13
CPI–λ-CG	25.94 ± 2.48	73.33 ± 6.67	86.72 ± 7.21	96.00 ± 0.00	190.31 ± 13.13
CPI (control)	90.62 ± 0.50	211.11 ± 10.18	73.76 ± 2.56	92.00 ± 0.00	247.19 ± 7.58

for individual CPI solutions (~96.5%) was significantly higher than for the mixed CPI–CG systems as soluble complexes ($p < 0.001$) (Table 1). CPI–κ-CG complexes showed greater solubility (~84.3%) than the other CG-types (ι-, λ-) ($p < 0.01$), which were similar in magnitude (~68.3% CPI–ι-CG; ~61.9% CPI–λ-CG; $p > 0.05$). As pH was lowered to 5.0, individual CPI solutions showed slightly reduced solubility (~90.6%) relative to that at higher pH, and to that of the mixed systems ($p < 0.001$) (Table 1). However, the solubility of insoluble complexes was reduced further, as strong electrostatic attraction between biopolymers resulted in precipitated structures. All three mixtures were found to be statistically different ($p < 0.001$), where CPI–ι-CG showed the greatest solubility (~61.9%), followed by κ-CG (~47.5%) and then λ-CG (~25.9%) (Table 1). The greater solubility of CPI–ι-CG over the other two CG types may be due to less interactions occurring between CPI and ι-CG, and therefore less precipitation out of solution, as evident by the CPI–ι-CG turbidity curve having a lower magnitude than the CPI–κ-CG or CPI–λ-CG curves (Fig. 2). Differences in order (based on solubility) within the mixed system as soluble and insoluble complexes is proposed to reflect difference in biopolymer mobility within the complexes during the process of forming the precipitate-type structures. Having reduced solubility at higher pHs within mixed systems is advantageous for protein separation applications. Klassen et al. (2011) and Liu, Elmer, Low, and Nickerson (2010) reported decreases in solubility at pH where insoluble complexes were formed in CPI–ι-CG and pea protein isolate–gum Arabic, respectively. Protein–polysaccharide complexes can also increase the solubility of the protein, particularly near its pI, as the polysaccharide acts to inhibit protein–protein aggregation (Ye, 2008). An increase in solubility at acidic pH (pH 4) has been found for soy protein isolate–chitosan complexes (Yuan et al., 2013). Burova et al. (2007) reported the addition of ι- and κ-CG increased the solubility of β-casein in the range of pH 3–5 where β-casein precipitates when alone in solution. The increase in solubility was more pronounced for κ-CG over ι-CG.

3.2.2. Foaming

Foam capacity (FC) reflects the amount of foam per amount of protein that can be generated upon application of mechanical shear. FC was found to decrease significantly at pH 6.75 for the mixed CPI–CG systems relative to individual CPI solutions (~271%) ($p < 0.001$). CPI–κ-CG soluble complexes (~144%) were found to be significantly higher than the other two types ($p < 0.001$), which were similar (~115%) ($p > 0.05$). As pH was lowered to 5.00, FC for individual CPI solutions was reduced (~211%) relative to that at higher pH (~271%), and for all mixed systems as well ($p < 0.001$) (Table 1). FC of insoluble complexes followed a similar trend as the soluble complexes, where CPI–κ-CG showed the higher FC (~98%) than the other two types ($p < 0.001$), whereas FC for CPI–ι-CG (~71%) and CPI–λ-CG (~73%) types was similar ($p > 0.05$) (Table 1). Reduced FC for the latter two types (CPI–ι-CG and CPI–λ-CG) relative to CPI–κ-CG complexes, between individual and mixed systems and between soluble and insoluble complexes is proposed to be associated with reduced solubility of the electrostatic complexes within the continuous phase. In order for FC to be high, the biopolymer must migrate to the air–water interface and unfold to expose hydrophobic groups towards the gaseous phase and hydrophilic groups to the aqueous phase to form a viscoelastic film around the air bubble. Electrostatic complexation is expected to influence both diffusion of proteins to that interface and re-alignment once there.

Foam stability relates to the degree of foam breakdown over a defined time period. At pH 6.75, FS was found to be relatively similar for the individual and all soluble CPI–CG complexes after 30 min, ranging between ~64 and 74% ($p > 0.05$; Table 1). However, as pH was reduced to 5.00, CPI–CG insoluble complexes showed slightly improved FS over the soluble complexes, whereas individual CPI solutions remained relatively unchanged. No statistical differences were apparent among the various CPI–CG insoluble complexes ($p > 0.05$) (Table 1). The slightly improved FC for the insoluble complexes is thought to be associated with increased continuous phase viscosity associated with precipitated complexes that remain within the interstitial phases of the form. Schmidt et al. (2010) reported that the addition of pectin to napin solutions led to improved FS relative to napin alone, where the authors thought improved FS was associated to with both unbound and bound proteins within the continuous phase that acted to delay liquid drainage from the foam structure. Miquelim, Lannes, and Mezzenga (2010) investigated FS of egg-albumin–κ-CG complexes relative to the albumin alone. The authors concluded the addition of κ-CG improved the FS by decreasing the surface tension to less than that of albumin alone, for pHs below the pI of albumin. Liu et al. (2010) found percent foam expansion to be similar for pea protein isolate alone and when complexed with gum Arabic regardless of pH. However the authors reported pea protein isolate FS to increase greatly with gum Arabic under pH conditions where complexation was occurring. This was hypothesized to be due to increased surface hydrophobicity of the pea protein isolate–gum Arabic complex over pea alone, leading to better adsorption and integration at the air–water interface and increased strength of the viscoelastic film due to the electrostatic interactions of the pea protein isolate–gum Arabic complexes.

3.2.3. Emulsification

The emulsification properties of soluble and insoluble complexes were evaluated in terms of their emulsion capacity (EC) and stability (ES) — by creaming. During emulsion formation, proteins and protein–polysaccharide complexes migrate to the oil–water interface, and then re-align to form a viscoelastic film around an oil droplet with hydrophobic residues oriented towards the oil phase and hydrophilic residues towards the aqueous phase (Walstra & van Vliet, 2008). Stability can be enhanced with increased electrostatic repulsion, steric hindrance between neighboring droplets and increased continuous phase viscosity (Walstra & van Vliet, 2008). Emulsion capacity refers to the amount of oil (g) a certain amount of protein (g) can support within an oil-in-water emulsion prior to inverting into a water-in-oil emulsion (Crenwelge, Dill, Tybor, & Landmann, 1974). At pH 6.75, CPI–CG soluble complexes showed reduced EC over the CPI control ($p < 0.001$) with CPI–κ-CG and CPI–ι-CG mixtures having greater EC than CPI–λ-CG

($p < 0.001$) (Table 1). In contrast, EC for all mixed systems was similar (~190 g/g) ($p > 0.05$) in their insoluble complex state (pH 5.00); however the EC for CPI alone was significantly higher (~247 g/g) ($p < 0.01$). Emulsion stability relates to the ability of an oil-in-water emulsion to resist gravitational phase separation as a consequence of droplet coalescence and creaming (McClements, 2007). Overall at pH 6.75, the ES for individual CPI and soluble CPI–CG complexes (regardless of type) was similar in magnitude ($p > 0.05$; Table 1). In contrast for ES data at pH 5.00, insoluble CPI–κ-CG and CPI–λ-CG complexes were found to be similar in magnitude (~96%, $p > 0.05$), but higher than that of CPI alone (~92%) ($p < 0.05$). Insoluble CPI–ι-CG complexes gave similar ES to that of CPI alone ($p > 0.05$). In the present study, surface charge of both individual CPI and mixed systems at pH 5.00 and 6.75 was relatively low (i.e., ~±20 mV) (Fig. 4); therefore its contribution to ES stability was quite low. At pH 5.00, solubility of the insoluble CPI–κ-CG and CPI–λ-CG complexes was lower compared to the individual CPI and CPI–ι-CG complexes, and as such most likely lead to slightly increased continuous phase viscosities resulting in the higher observed emulsion stability data.

Gu et al. (2005) reported that under conditions where weak complexes were formed between β-lactoglobulin and CG the order of creaming stabilities was κ-CG > ι-CG > λ-CG. In a β-lactoglobulin–CG system at pH where strong electrostatic interactions were occurring no differences were found for creaming stabilities between the three CG types below a critical CG concentration (Gu et al., 2005). Uruakpa and Arntfield (2005) found that adding κ-CG to CPI, at pH where the biopolymers were oppositely charged, increased the emulsion stability of CPI. Stone and Nickerson (2012) reported that an increase in WPI emulsion stability when complexed with CG may be due to charge repulsion between droplets, viscoelastic film formation with protein–polysaccharide complexes saturating the oil–water interface and steric stabilization caused by the CG chains. Li, Fang, Al-Assaf, Phillips, and Jiang (2012) reported that bovine serum albumin (BSA)–sugar beet pectin either increased or decreased emulsion stability depending on the level of interactions occurring between the protein and polysaccharide. At increased pHs where little to no complexation was taking place no increase in emulsion stability was found due to depletion flocculation and competitive adsorption. Under conditions where soluble BSA–pectin complexes were formed an increase in emulsion stability was found which the authors attributed to the thick protein–polysaccharide layer at the interface causing strong steric stabilization of the droplets. And finally insoluble BSA–pectin complexes led to extremely unstable emulsions due to bridging flocculation.

4. Conclusion

The formation of soluble and insoluble complexes was investigated in CPI–(κ-, ι- and λ-type) CG mixtures as a function of pH and biopolymer mixing ratio. Complexes formed at pHs > pI and critical pHs plateaued at a 15:1–20:1 CPI–CG mixing ratio. CPI–CPI aggregates were thought to be formed based on the pH dependence of pH_c. Complex formation between CPI and (κ-, ι- and λ-type) CG was found to have a significant negative effect on solubility, foaming capacity, and emulsion capacity at pHs where soluble (pH 6.75) and insoluble (pH 5.00) complexes exist, whereas the foaming stability and emulsion stability properties of CPI were similar or increased with the addition of CG at these pHs. Increases in foam and emulsion stability are mostly likely associated with an increase in the continuous phase viscosities. Within the mixed systems CPI–κ-CG had the greatest FC at pHs where soluble and insoluble complexes exist and CPI–λ-CG had significantly less EC and solubility than the other CG types at pH corresponding to the presence of soluble complexes. Overall, complexation-induced changes to protein solubility offered the most dramatic results of all the functionality tests measured, with possible applications in protein (or other charged particles) separation techniques where precipitation is desired.

Acknowledgments

Financial support for this research was provided by the Saskatchewan Canola Development Commission and the Saskatchewan Agriculture Development Fund.

References

Aider, M., & Barbana, C. (2011). Canola proteins: Composition, extraction, functional properties, bioactivity, applications as a food ingredient and allergenicity — A practical and critical review. *Trends in Food Science and Technology*, *22*, 21–39.

AOAC (2003). *Official method of analysis* (17th ed.)Virginia: Association of Official Analytical Chemists, Inc.

Berot, S., Compoint, J. P., Larre, C., Malabat, C., & Gueguen, J. (2005). Large scale purification of rapeseed proteins (*Brassica napus* L.). *Journal of Chromatography B*, *818*, 35–42.

Boral, S., & Bohidar, H. B. (2010). Effect of ionic strength on surface-selective patch binding-induced phase separation and coacervation in similarly charged gelatin–agar molecular systems. *The Journal of Physical Chemistry. B*, *114*, 12027–12035.

Burova, T. V., Grinberg, N. V., Grinberg, V. Y., Usov, A. I., Tolstoguzov, V. B., & de Kruif, C. G. (2007). Conformational changes in ι- and κ-carrageenans induced by complex formation with bovine β-casein. *Biomacromolecules*, *8*, 368–375.

Clark, A. H., & Ross-Murphy, S. B. (1987). Structural and mechanical properties of biopolymer gels. *Advances in Polymer Science*, *83*, 57–192.

Crenwelge, D. D., Dill, C. W., Tybor, T. B., & Landmann, W. A. (1974). A comparison of the emulsification capacities of some protein concentrates. *Journal of Food Science*, *39*(1), 175–177.

de Vries, R., Weinbreck, F., & de Kruif, C. G. (2003). Theory of polyelectrolyte adsorption on heterogeneously charged surfaces applied to soluble protein–polyelectrolyte complexes. *Journal of Chemical Physics*, *118*, 4649–4659.

Dickinson, E. (1998). Stability and rheological implications of electrostatic protein–polysaccharide interactions. *Trends in Food Science and Technology*, *9*, 340–349.

Folawiyo, Y. L., & Apenten, R. K. O. (1996). Effect of pH and ionic strength on the heat stability of rapeseed 12S globulin (cruciferin) by the ANS fluorescence method. *Journal of the Science of Food and Agriculture*, *70*, 241–246.

Girard, M., Sanchez, C., Laneuville, S. I., Turgeon, S. L., & Gauthier, S. F. (2004). Associative phase separation of β-lactoglobulin/pectin solutions: A kinetic study by small angle static light scattering. *Colloids and Surfaces. B, Biointerfaces*, *35*(1), 15–22.

Gu, Y. S., Decker, E. A., & McClements, D. J. (2005). Influence of pH and carrageenan type on properties of β-lactoglobulin stabilized oil-in-water emulsions. *Food Hydrocolloids*, *19*, 83–91.

Gupta, A. N., Bohidar, H. B., & Aswal, V. K. (2007). Surface patch binding induced intermolecular complexation and phase separation in aqueous solutions of similarly charged gelatin–chitosan molecules. *The Journal of Physical Chemistry. B*, *111*, 1137–10145.

Klassen, D. R., Elmer, C. M., & Nickerson, M. T. (2011). Associative phase separation involving canola protein isolate with both sulphated and carboxylated polysaccharides. *Food Chemistry*, *126*(3), 1094–1101.

Klemmer, K. J., Waldner, L., Stone, A., Low, N. H., & Nickerson, M. T. (2012). Complex coacervation of pea protein isolate and alginate polysaccharides. *Food Chemistry*, *130*(3), 710–715.

Lampart-Szczapa, E. (2001). Legume and oilseed proteins. In Z. E. Sikorski (Ed.), *Chemical and functional properties of food proteins* (pp. 407–436). New York: CRC Press.

Li, X., Fang, Y., Al-Assaf, S., Phillips, G., & Jiang, F. (2012). Complexation of bovine serum albumin and sugar beet pectin: Stabilising oil-in-water emulsions. *Journal of Colloid and Interface Science*, *388*, 103–111.

Liu, S., Cao, Y. L., Ghosh, S., Rousseau, D., Low, N. H., & Nickerson, M. T. (2010). Intermolecular interactions during complex coacervation of pea protein isolate and gum Arabic. *Journal of Agricultural and Food Chemistry*, *58*, 552–556.

Liu, S., Elmer, C., Low, N. H., & Nickerson, M. T. (2010). Effect of pH on the functional behaviour of pea protein isolate–gum Arabic complexes. *Food Research International*, *43*, 489–495.

Liu, S., Low, N. H., & Nickerson, M. T. (2009). Effect of pH, salt, and biopolymer ratio on the formation or pea protein isolate–gum Arabic complexes. *Journal of Agricultural and Food Chemistry*, *57*, 1521–1526.

McClements, D. J. (2007). Critical review of techniques and methodologies for characterization of emulsion stability. *Critical Reviews in Food Science and Nutrition*, *47*, 611–649.

Miquelim, J. N., Lannes, S. C. S., & Mezzenga, R. (2010). pH influence on the stability of foams with protein–polysaccharide complexes at their interfaces. *Food Hydrocolloids*, *24*, 398–405.

Monsalve, R. I., & Rodriguez, R. (1990). Purification and characterization of proteins from the 2S fraction from seeds of the Brassicaceae family. *Journal of Experimental Botany*, *41*, 89–94.

Morr, C. V., German, B., Kinsella, J. E., Regenstein, J. M., Van Buren, J. P., Kilara, A., et al. (1985). A collaborative study to develop a standardized food protein solubility procedure. *Journal of Food Science*, *50*(6), 1715–1718.

Morris, E. R., Rees, D. A., & Robinson, G. (1980). Cation-specific aggregation of carrageenan helices: Domain model of polymer gel structure. *Journal of Molecular Biology*, *138*, 349–362.

Piculell, L. (2006). Gelling carrageenans. In A. M. Stephen, G. O. Philips, & P. A. Williams (Eds.), *Food polysaccharides and their applications* (pp. 239–287). Boca Raton: CRC Press.

Schmidt, I., Novales, B., Boue, F., & Axelos, M. A. V. (2010). Foaming properties of protein/pectin electrostatic complexes and foam structure at nanoscale. *Journal of Colloid and Interface Science*, *345*, 316–324.

Schmitt, C., Sanchez, C., Desobry-Banon, S., & Hardy, J. (1998). Structure and technofunctional properties of protein–polysaccharide complexes: A review. *Critical Reviews in Food Science and Nutrition*, *38*, 689–753.

Schmitt, C., & Turgeon, S. L. (2011). Protein/polysaccharide complexes and coacervates in food systems. *Advances in Colloid and Interface Science*, *167*, 63–70.

Semenova, M. G., Pavlovskaya, G. E., & Tolstoguzov, V. B. (1991). Light scattering and thermodynamic phase behavior of the system 11S globulin–κ-carrageenan–water. *Food Hydrocolloids*, *4*, 469–479.

Singh, S. S., Siddhanta, A. K., Meena, R., Prasad, K., Bandyopadhyay, S., & Bohidar, H. B. (2007). Intermolecular complexation and phase separation in aqueous solutions of oppositely charged biopolymers. *International Journal of Biological Macromolecules*, *41*, 185–192.

Stone, A. K., & Nickerson, M. T. (2012). Formation and functionality of whey protein isolate–(kappa-, iota-, and lambda-type) carrageenan electrostatic complexes. *Food Hydrocolloids*, *27*, 271–277.

te Nijenhuis, K. (1997). Thermoreversible networks: Viscoelastic properties and structure of gels. *Advances in Polymer Science*, *130*, 1–267.

Tolstoguzov, V. B. (1991). Functional properties of food proteins and role of protein–polysaccharide interaction. *Food Hydrocolloids*, *4*, 429–468.

Tolstoguzov, V. B. (2002). Thermodynamic aspects of biopolymer functionality in biological systems, foods, and beverages. *Critical Reviews in Biotechnology*, *22*, 89–174.

Uruakpa, F. O., & Arntfield, S. D. (2005). Emulsifying characteristics of commercial canola protein–hydrocolloid systems. *Food Research International*, *38*, 659–672.

Walstra, P., & van Vliet, T. (2008). Dispersed systems: Basic considerations. In S. Damordaran, K. L. Parkin, & O. R. Fennema (Eds.), *Fennema's food chemistry* (pp. 783–847) (4th ed.). Boca Raton: CRC Press.

Weinbreck, F., Nieuwenhuijse, H., Robijn, G. W., & de Kruif, C. G. (2003). Complex formation of whey proteins: Exocellular polysaccharide EPS B40. *Langmuir*, *19*, 9404–9410.

Weinbreck, F., Nieuwenhuijse, H., Robjin, G. W., & de Kruif, C. G. (2004). Complexation of whey proteins with carrageenan. *Journal of Agricultural and Food Chemistry*, *52*, 3550–3555.

Wu, J., & Muir, A. D. (2008). Comparative structural, emulsifying, and biological properties of 2 major canola proteins, cruciferin and napin. *Journal of Food Science*, *73*, 210–216.

Xia, J., & Dubin, P. L. (1994). Macromolecular complexes in chemistry and biology. In P. L. Dubin, J. Bock, R. Davis, D. N. Shultz, & C. Thies (Eds.), Berlin: Springer-Verlag.

Xu, Y., Mazzawi, M., Chen, K., Sun, L., & Dubin, P. L. (2011). Protein purification by polyelectrolyte coacervation: Influence of protein charge anisotropy on selectivity. *Biomacromolecules*, *12*, 1512–1522.

Ye, A. (2008). Complexation between milk proteins and polysaccharides via electrostatic interaction: Principles and applications — A review. *International Journal of Food Science and Technology*, *43*, 406–415.

Yuan, Y., Wan, Z. -L., Yin, S. -W., Yang, X. -Q., Qi, J. -R., Liu, G. -Q., et al. (2013). Characterization of complexes of soy protein and chitosan heated at low pH. *LWT-Food Science and Technology*, *50*, 657–664.